1

Solar Wind Laws Valid for any Phase of a Solar Cycle

V.G. Eselevich
Institute of Solar-Terrestrial Physics of Siberian Branch of Russian Academy of Sciences, Irkutsk Russia

1. Introduction

First, let us remind what a physical law is.

It is an empirically established, formulated strictly in words or mathematically, stable relation between repetitive phenomena and states of bodies and other material objects in the world around. Revealing physical regularities is a primary objective of physics. A physical law is considered valid if it has been proved by repeated experiments. A physical law is to be valid for a large number of objects; ideally, for all objects in the Universe. Obviously, the last requirement is especially difficult to test. We will, therefore, somewhat confine ourselves to the following comments:

a. We will lay down only SW physical laws, calling them simply "laws". Here, we will take into account that they meet the main above-stated requirements for physical laws.
b. Any law is fulfilled under ideal conditions, i.e., when its effect is not violated by outside influence. For instance, the Newton first law of motion may be tested only when the friction force is absent or tends to zero. Since SW conditions are often far from ideal, it is sometimes difficult to determine, lay down, and prove the existence of an SW physical law.
c. We will distinguish between the laws and their mechanisms of effect. For example, the law of universal gravitation is well known, but its mechanism is still unclear.
d. Obviously, the relevance of these laws is different. But all of them are of limited application. To illustrate, laws of simple mechanics are violated for relativistic velocities or superlarge masses of substance. The Ohm's law is valid only if there is current in the conductor. The SW laws are valid only for a hot ionised medium, etc.
e. It is good to keep in mind that a part of the SW laws defined below may later merge into one law. Time will show. As for now, considering the SW laws separately is reasonable, because in this way we can examine their mechanisms that are likely to be different.

Laying down SW laws actually implies that the "solar wind" subdiscipline of space science turns from multidirectional investigations and data collection into an independent branch of physics. This, based on established laws, provides a way to examine the SW behaviour in more complex situations, when it is under the effect of several factors at once, without resorting to statistical methods that are not capable of restoring the truth.

Laying down a law enables us to pose tasks of examining its mechanism as well as to discover new laws rather than repeating and rechecking well-known ones.

Knowing SW laws is of critical importance for developing a unified theory of SW that is practically absent now. The point is that SW obeys the diluted plasma dynamics laws with due regard to boundary conditions: on the one hand, it is the Sun; on the other, it is the galactic environment. The distance between the galactic environment and the Sun is $R \sim 2 \bullet 10^4$ R_0 (R_0 is the solar radius); the SW density decreases by law of $(R/R_0)^2$ (i.e., $\sim 4 \bullet 10^8$ times). Thus, for SW at distances of order and less than the Earth's orbit ($R \approx 214 R_0$), the infinity condition is simple: SW density tends to zero. However, the conditions on the Sun are totally determined by the experimentally established SW laws comprising such notions as coronal holes, bases of the coronal streamer belt, active regions, and magnetic tubes emerging from the solar convective zone - these are the sources of various SW on the Sun without knowledge of which it is impossible to impose boundary conditions there.

The sequence of the presentation is as follows: a brief wording of a law and then a reference to 2-4 first fundamental papers on this law according to their time priority (in some cases, more references will be given). They are in bold typed in the text, their authors are bold typed. For some laws we will explain their possible violations under the influence of other factors as well as possible problems associated with their implementation mechanisms.

I took the liberty of naming some SW laws, where considered it possible and important, after their discoverers, for example:

The Law of the Solar Wind (SW) Existence - the **Ponomarev-Parker Law;**
The Law of the Existence of Collisionless Shocks in the Diluted Plasma – the **Sagdeev Law**;
The Law of Two Mechanisms for Accelerating Solar Energetic Particles – the **Reams Law**.
The Law of the Relation between the Type-II Radio Emission and Collisionless Shocks - the **Zheleznyakov-Zaitsev Law**

2. Quasi-stationary solar wind laws

Law 1. "Of the solar wind (SW) existence": There is a diluted plasma stream – solar wind (SW) – from the Sun.

This law was theoretically substantiated in (**Ponomarev, 1957; Vsekhcvyatcky, et al., 1957; Parker, 1958)**. They predicted the SW existence in the Earth's orbit based on the well-known high temperature of the coronal plasma that provided plasma acceleration due to pressure gradient forces.

The SW stream existence was confirmed by experiments at the Luna-2 and Luna-3 Automatic Interplanetary Stations (**Gringauz, et al., 1960**) and the Explorer-10 satellite (**Bonetti et al., 1963**).

However, Ponomarev and Parker failed to answer the question about the mechanism of the SW origin near the solar surface where the temperature is within 6000 degrees (i.e., how the plasma from the solar surface enters the corona). That is precisely why the Ponomarev-Parker law opened a new chapter in solar-terrestrial physics research that has been over half a century already.

Further investigations demonstrated that there are mostly three SW types (V.G. Eselevich, et al., 1990; Schwenn and Marsch, 1991; McComas et al, 2002): two quasi-stationary SW types with fairly long-lived sources on the Sun (over 24 hours, often weeks and even months): **the fast SW** (its maximum velocity V_M is 450-800 km/s) flowing out of coronal holes (CH), and **the slow SW** (its maximum velocity is 250-450 km/s) flowing out of the coronal streamer belt or chains (pseudostreamers). The third type is **the sporadic SW**. Its sources on the Sun exist less than 24 hours (flares, coronal mass ejections (CME), eruptive prominences).

The three SW types have different generation mechanisms that are still unclear. Therefore, their associated laws are laid down separately.

Law 2. "Fast SW": the sources of the fast SW on the Sun are coronal holes. The maximum SW velocity V_M in the Earth's orbit is related to the area (S) of a coronal hole, enclosed in the latitude range λ = ±10° relative to the ecliptic plane (Fig. 1), by V_M (S)=(426±5) + (80±2)·S at S≤5•10^{10} km^2 and V_M (S) ≈ const ≈ 750-800 km/s at S>5•10^{10} km^2.

This law was experimentally established in (**Nolte et al., 1976**), where six equatorial coronal holes were recorded in soft X-ray concurrently with time velocity profiles of fast SW streams in the Earth's orbit during ten Carrington rotations. It was verified by many subsequent investigations both for equatorial coronal holes and for extra equatorial ones, in particular:

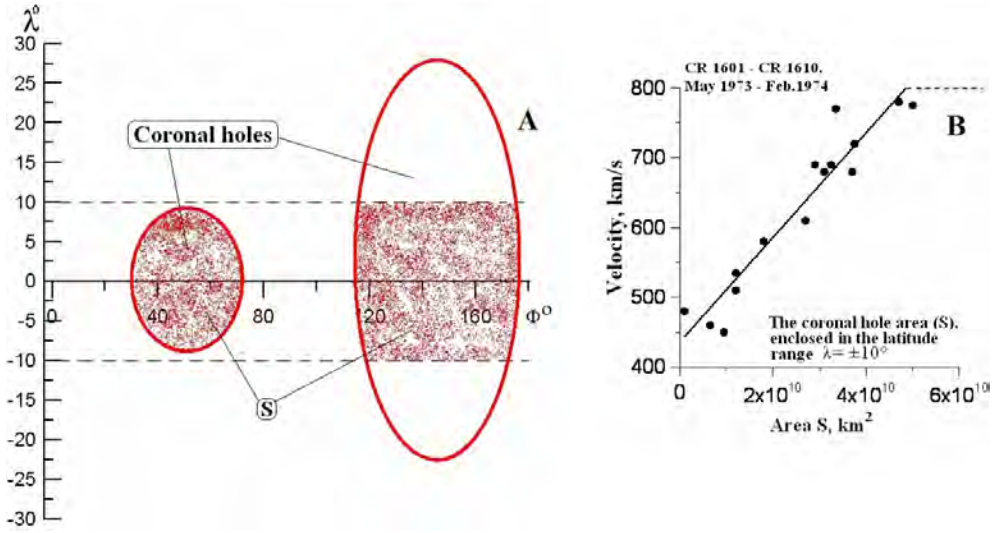

Fig. 1. Two different-size subequatorial coronal holes. Red CH areas are those located at latitudes λ within ±10° relative to the equatorial plane.

a. according to the Ulysses measurements, the maximum velocity V_M of the SW streams from the polar coronal holes, whose area S>5•10^{10} km^2, was V_M ≈ const ≈750-800 km/s (Goldstein et al.,1996).
b. The dependence V_M(S) on Law 2 was used to develop a method to compute the V(t) profile for the fast SW in the Earth's orbit from characteristics of any coronal holes (equatorial and off-equatorial) (V.G. Eselevich, , 1992 ; V.G. Eselevich, V. & M. V.

Eselevich, 2005). It provided a basis for the continuous website comprising the prediction of V(t) for the fast SW. The comparison between the predicted results at this website and experimental curves of V(t) over several years demonstrated high efficiency and validity of this method (Eselevich, et al., 2009).

c. Another independent method of testing Law 2 is the dependence of the superradial divergence "f" of magnetic field lines emanating from a coronal hole with maximum velocity V_M of the fast SW. This dependence was obtained in (V.G. Eselevich & Filippov, 1986; Wang, 1995). On its basis, another method to compute the V(t) profile for the fast SW in the Earth's orbit from characteristics of coronal holes (equatorial and off-equatorial) has been developed (Wang & Sheeley,1990; Arge & Pizzo, 2003). A website to predict V(t) profiles of fast SW streams in the Earth's orbit using this method (the V(f) dependence at the base of coronal holes) has been functioning continuously for many years. The method provides results in their reliability and validity close to the prediction method using the $V_M(S)$ dependence (Eselevich et al., 2009).

Since the value "f" is, in turn, a function of S (V.G. Eselevich & Filippov, 1986), the results of this method also support Law 2.

Law 3. "Streamer belts": the streamer belt with the slow SW in the Earth's orbit is recorded as areas with higher plasma density containing an odd number of the interplanetary magnetic field (IMF) sign changes or an IMF sector boundary.

Svalgaard et al. (1974) showed that the streamer belt separates areas with an opposite direction of the global magnetic field radial component on the solar surface. It means that at the base of the streamer belt there are magnetic field arcs along whose tops there goes a neutral line of the Sun's global magnetic field radial component (dashed curve in Fig. 2A). The intersections of the neutral line with the ecliptic plane (red horizontal line in Fig. 2A) are recorded in the Earth's orbit as sector boundaries of the interplanetary magnetic field (IMF) (arrow "sec" in Fig. 2B) (**Korzhov, 1977**).

All this was verified and developed in many subsequent studies (e.g., Gosling et al., 1981; Burlaga et al., 1981; Wilcox & Hundhausen, 1983; Hoeksema, 1984).

Law 4. "Streamer chains (or pseudostreamer)": Streamer chains with the slow SW in the Earth's orbit are recorded as areas with higher plasma density that contain an even number of IMF sign changes.

In (**V.G. Eselevich et al., 1999**) it was demonstrated that, except the streamer belt proper, there are its branches termed streamer chains. The chains in the white-light corona look like the belt itself - like areas with higher brightness. There is slow SW in them; its properties are approximately identical to those in the streamer belt. However, the chains differ from the belt in that they separate open magnetic field lines in the corona with identical magnetic polarity. Thus, the magnetic field structures, calculated in potential approximation, at the base of the chains have the form of double arches (in general case - an even number of arches), as opposed to the streamer belt where there are single arches at the base (an odd number of arches), see Fig. 2A. The properties of the streamer chains have been poorly studied so far; their name has not been established. So, in the very first paper (**V.G. Eselevich & Fainshtein, 1992**), they were termed "heliospheric current sheet without a neutral line" (HCS without NL); in (Zhao & Webb, 2003), "unipolar closed field region" (the streamer belt in that paper was termed "bipolar closed field region"). In the most recent

investigations (Wang et al., 2007), they were termed pseudostreamers. In (Ivanov et al., 2002), manifestations of the chains in the heliosphere were designated as subsector boundaries. We will use the term "'streamer chains", and their manifestations in the Earth's orbit will be termed as subsector boundaries (arrow "subsec" in Fig. 2B).

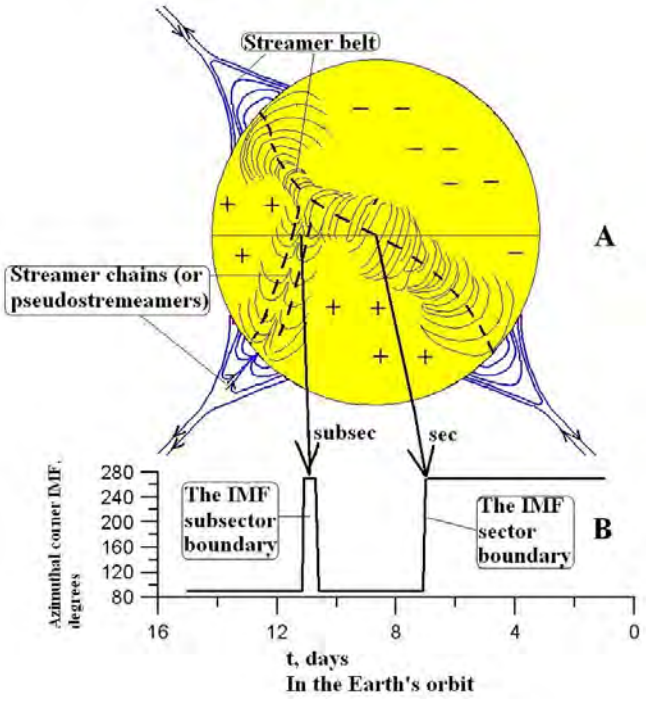

Fig. 2. A) The coronal streamer belt and chains separating, respectively, areas on the solar surface with opposite and equal direction of the Sun's global magnetic field radial component. The single dash is the neutral line (NL) of the magnetic field radial component passing through the tops of the magnetic field arcs at the base of the streamer belt. The double dash is two NLs along double magnetic field arcs at the base of the streamer chains. B) The IMF azimuthal angle distribution in the Earth's orbit on the solar surface. It corresponds to that in (A).

Law 5. "Interaction between fast and slow SWs" In the heliosphere, there is a region of collision between slow and fast SWs caused by solar rotation. Inside the region, slow and fast SW streams are separated by a thin surface termed interface.

It has been shown theoretically (**Dessler & Fejer, 1963; Hundhausen & Burlaga, 1975**) and experimentally (**Belcher & Davis, 1971; Burlaga, 1974**) that the radially propagating fast and slow SWs collide in the heliosphere (in the Earth's orbit, in particular) starting with $R>20R_0$ and on, owing to the solar rotation (the fast SW overtakes the slow one). Between them, at the fast SW front, develops a sharp boundary less than $\approx 4 \cdot 10^4$ km thick. It is termed interface. The longitudinal proton temperature and the radial and azimuthal SW velocities abruptly increase at the interface; the proton density abruptly decreases (Gosling et al.,

1978). Also, electron temperature, relative portion of alpha particles, alpha-particles velocity relative to protons (Gosling et al., 1978; Borrini et al., 1981), ratio of ion content O^{7+}/O^{6+} reflecting the coronal temperature, and Mg/O controlled by the FIP effect (Geiss et al., 1995) abruptly increase at the interface, while the flow of matter j = NV decreases. A valid parameter enabling separating the flows of these two types is an entropy in the form of $S = k \ln(T/N^{0.5})$ (Burton et al., 1999). Here, in the gas entropy formula, it is assumed that the polytropic index $\gamma = 1.5$. The well-defined difference in entropy between these two streams enables us to record the so-called trailing interface located at the trailing edge solar wind stream. The trailing interface separating the fast SW from the following slow SW differs from the interface at the front of the following fast SW and is likely to be somewhat thicker.

Thus, the time variation in the entropy allows to unambiguously separate any fast SW from the ambient slow SW (and vice versa). The sharp difference in the said parameters and, especially, in the entropy suggests that the genesis for these two types of SW streams is different.

Law 6. "Nonradialities of rays of the streamer belt and chains": Nonradiality of rays $\Delta\lambda$ of the streamer belt and chains depends on the latitude of λ_0 of their location near the Sun and peaks at $\lambda_0 \approx \pm 40°$.

The cross-section of the streamer belt in white light is a helmet-shaped base resting on the solar surface and extending upward as a radially oriented ray (solid curves in Fig. 3A). Inside the helmet, there may be loop structures of three types: I and II in Fig. 3A correspond to the streamer belt splitting up the regions of the radial global magnetic field component with opposite polarity (an odd number of loops under the helmet); type III corresponds to the streamer chains splitting up the regions with identical radial component polarity (an even number of loops). Type II is largely observed around the minimum and at the onset of an increase in solar activity at $\lambda_0 \approx 0°$. The symbol λ_0 denotes the latitude of the helmet base centre near the solar surface. The latitude of the helmet centre and, then, of the ray to which the helmet top transforms changes usually with distance away from the solar surface (dashed line in Fig.3 (I)). And only at R > 5Ro, the ray becomes radial, but its latitude (designated λ_E) may differ greatly from the initial latitude of λ_0 at the helmet base. The latitude change is an angle $\Delta\lambda$. A positive $\Delta\lambda$ corresponds to the equatorward deviation; a negative $\Delta\lambda$ corresponds to the poleward one. To exclude the necessity of considering the sign in Fig. 3B, we defined the deviation as: : $\Delta\lambda = |\lambda_0| - |\lambda_E|$ (i.e., equally for the Northern and Southern hemispheres).

The analysis of the measurements and the plot in Fig. 3 suggests that at R < 5Ro from the solar centre (**V.G.Eselevich & M.V. Eselevich, 2002**):

- the deviation of the higher brightness rays from the radial direction is equatorward for the latitude range up to $\approx \pm 60^o$, nearly identical in the Northern and Southern hemispheres (curve in Fig. 3B), and is slightly asymmetric relative to the axis $\lambda_0 \approx 0°$) when observed at the western and eastern limbs in the streamer belt and chains;
- the deviation value $\Delta\lambda$ unambiguously depends on the latitude of the ray λ_0 near the solar surface;
- the near-equatorial rays almost do not deviate from the radial direction ($\lambda_0 \approx 0°$) .

These conclusions were then confirmed in the investigations based on the extensive statistics for the complete solar cycle in (**Tlatov & Vasil'eva, 2009**).

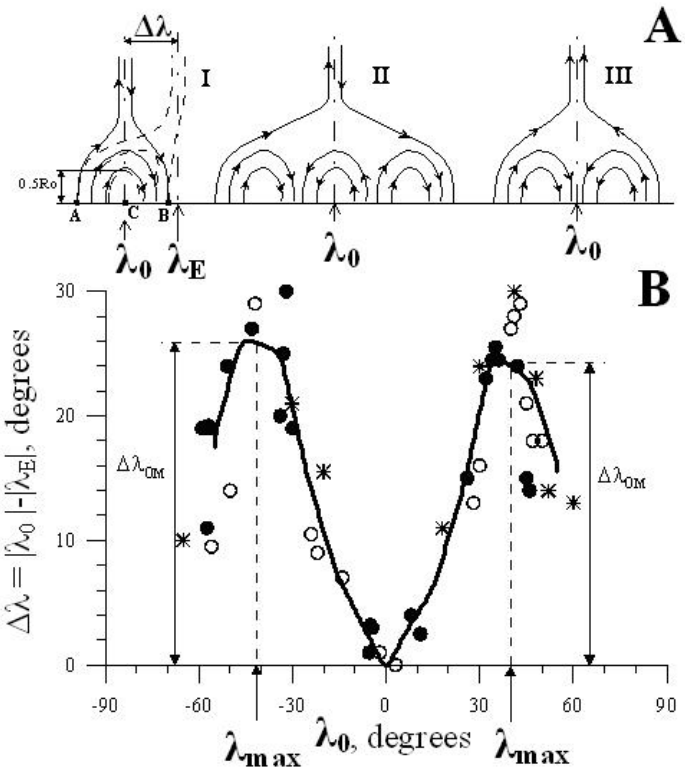

Fig. 3. A) The idealized magnetic field lines in the hamlet with a ray based on it: I and II in the streamer belt, III - in streamer chains. The dash in I indicates the pattern accounting for the streamer nonradiality effect. B) The dependence of the total angular deviation $\Delta\lambda$ on latitude λ_0 for 51 streamer belt brightness rays (black circles are the W limb; light circles, the E limb) and streamer chains (stars) over the period November 1996 through June 1998 as deduced from LASCO C1 and C2 data **(V.G. Eselevich & M.V. Eselevich, 2002**).

The mechanism for the emergence of the ray nonradiality in the streamer belt and chains has been still unclear, but the law itself is the basis for testing any theory about the solar wind origin.

Law 7. "Of the streamer belt ray structure": The coronal streamer belt is a sequence of pairs of higher brightness rays (or two, closely spaced ray sets). Ray brightnesses in each pair may differ in general case. The neutral line of the radial component of the Sun's global magnetic field goes along the belt between the rays of each of these pairs.

The first experimental evidence for the existence of the coronal streamer belt regular ray structure was obtained in (**V.G. Eselevich & M.V. Eselevich, 1999**). Later, more detailed investigations carried out in (**V.G. Eselevich & M.V. Eselevich, 2006**) revealed that the spatial streamer belt structure has the form of two closely-spaced rows of higher brightness rays (magnetic tubes with SW plasma moving in them) separated by the neutral line of the global magnetic field radial component (Fig. 4a). Figure 4b shows the belt cross-section in the form of two rays enveloping the helmet on either side. The magnetic field direction

(arrows and + - signs) in these rays is opposite. The pattern does not show the nonradiality of the rays in the streamer belt plane near the solar surface at R< 4-5Ro.

The double-ray streamer belt structure was considered as a result of the instability development. In the streamer belt type current systems, there is a proton "beam" relative to the main SW mass along the magnetic field (Schwenn & Marsch, 1991). In (**Gubchenko et al., 2004)**, in the context of the kinetic approach, it was shown that the sequences of magnetic tube (ray) pairs analogous to those observed above may be formed along the belt due to exciting the "stratification modes" of oscillations. If it is true, then we deal with collective properties of diluted plasma that manifest themselves in forming cosmic-scale structures.

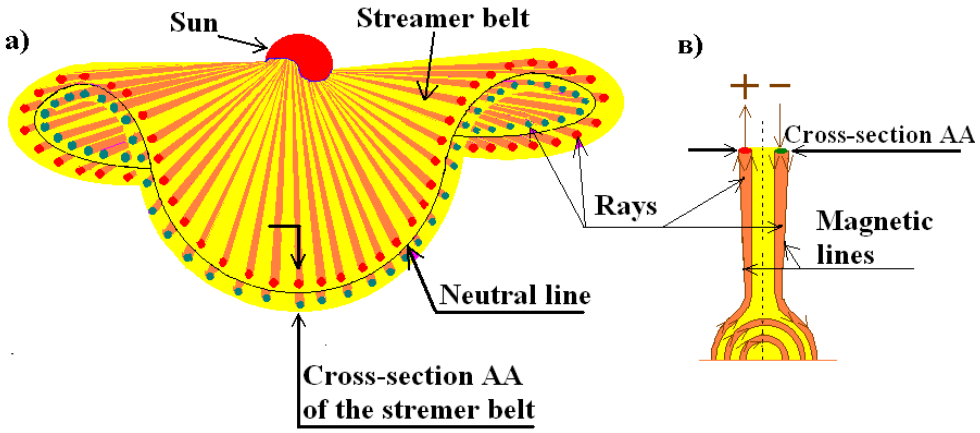

Fig. 4. The spatial ray structure of the coronal streamer belt (a); the streamer belt cross-section (AA) (b). In red rays of the top row of the streamer belt, the magnetic field is directed from the Sun (+); in green rays of the bottom row, to the Sun (–). The neutral line between rays (solid line).

We note that although the theoretically considered possible mechanism for the formation of the streamer belt ray structure yields the result qualitatively consistent with the experiment, the true cause of this very interesting phenomenon is still far from clear.

Law 8. "Of the heliospheric plasma sheet structure": The cross-section of the heliospheric plasma sheet (HPS) in the Earth's orbit generally takes the form of two density maxima of a characteristic size ≈2°-3° (in the heliospheric coordinate system) with a sector boundary between them. Such a structure is quasistationary (remains unchanged for nearly 24 hours). HPS is an extension of the coronal streamer belt structure (ray structure) into the heliosphere.

The streamer belt extension into the heliosphere is termed a heliospheric plasma sheet (HPS) (Winterhalter, et al., 1994) According to the findings of (Borrini, et al., 1981;V.G. Eselevich and Fainshtein, 1992), the quasistationary slow SW flowing into HPS in the Earth's orbit is characterised by the following parameters and features:

- a relatively low SW velocity V ≈ 250 - 450 km/s (the maximum velocity in the fast SW flowing out of coronal holes V ≈ 450 - 800 km/s);

- an enhanced plasma density with maximum values N_{max}>10 cm^{-3} (in the fast SW, Nmax <10 cm^{-3});
- anticorrelation of profiles of plasma density N(t) and of the magnetic field module B(t) on time scales of order of hours and more;
- a lower proton temperature Tp < 10^5 ^oK;
- one or several (an odd number) IMF sign reversals is the characteristic feature of the sector boundary or its structure.

The availability of all these signs is enough to unambiguously determine the heliospheric plasma sheet in the Earth's orbit.

According to (**Bavassano, et al., 1997**), the HPS cross-section is a narrow (with an angular size of ≈ 2^o -3^o) peak of plasma density with the built-in IMF sector boundary and is a sufficiently stable structure throughout the way from the Sun to the Earth (the pattern in Fig. 5A).

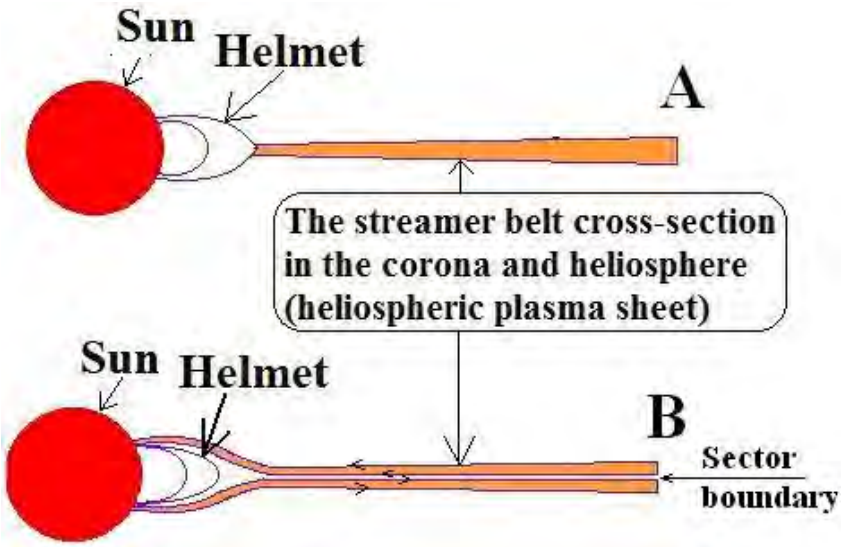

Fig. 5. The streamer belt cross-section structure in the corona and heliosphere (heliospheric plasma sheet) according to the results obtained in **(Bavassano, et al., 1997)** (A) and **(V.G. Eselevich & M.V. Eselevich, 2007b)** (B).

The HPS cross-section improved structure obtained in (**V.G. Eselevich, V. & M.V. Eselevich, 2007b**) proved to be slightly different from that in (**Bavassano, et al., 1997**) in the following characteristics:

a. The streamer belt cross-section in the corona and heliosphere is, in general case, two closely-spaced rays with identical or different values of density peaks, not one ray as it is assumed in (**Bavassano, et al., 1997**). The sector boundary is between the density peaks. One ray is observed, when the density peak of one ray is much *smaller* than that of the other (the pattern in Fig. 5B).
b. Rays do not start at the helmet top (like in the upper panel of Fig. 5A) but on the solar surface (Fig. 5B).

Mechanisms generating the slow SW in the streamer belt rays have been still unclear and are the subject for future research.

Laws 7 and 8 may later merge.

Law 9. "Of the heliospheric plasma sheet fractality": The fine structure of the heliospheric plasma sheet in the Earth's orbit is a sequence of nested magnetic tubes (fractality). Sizes of these tubes change by almost two orders of magnitude as they nest.

Analysing the data from the Wind and IMP-8 satellites has revealed that the slow SW in the heliospheric plasma sheet is a set of magnetic tubes containing plasma of an enhanced density (Nmax > 10 cm^{-3} in the Earth's orbit) that are the streamer belt ray structure extension into the heliosphere (**M.V. Eselevich & V.G. Eselevich, 2005**) (Fig. 6). Each tube has a fine structure in several spatial scales (fractality) from ≈ 1.5^o -3^o (in the Earth's orbit this equals to 2.7 -5.4 hours or (4-8)·10^6 km) to the minimum ≈ 0.03^o -0.06^o, i.e., angular sizes of nested tubes change by almost two orders of magnitude. In each spatial scale under observation, the magnetic tubes are diamagnetic (i.e., there is a diamagnetic (drift) current on their surface, decreasing the magnetic field inside the tube and increasing it outside). As this takes place, $\beta = 8\pi \cdot [N(Te + Tp)]/ B^2$ inside the tube is greater than β outside. In many cases, the total pressure $P = N(Te + Tp) + B^2/8\pi$ is practically constant both inside and outside the tubes in any of the above scales. The magnetic tubes are quasi-stationary structures. The drift (or diamagnetic) current at the tube boundaries is stable relative to the excitation of random oscillations in magnetised plasma.

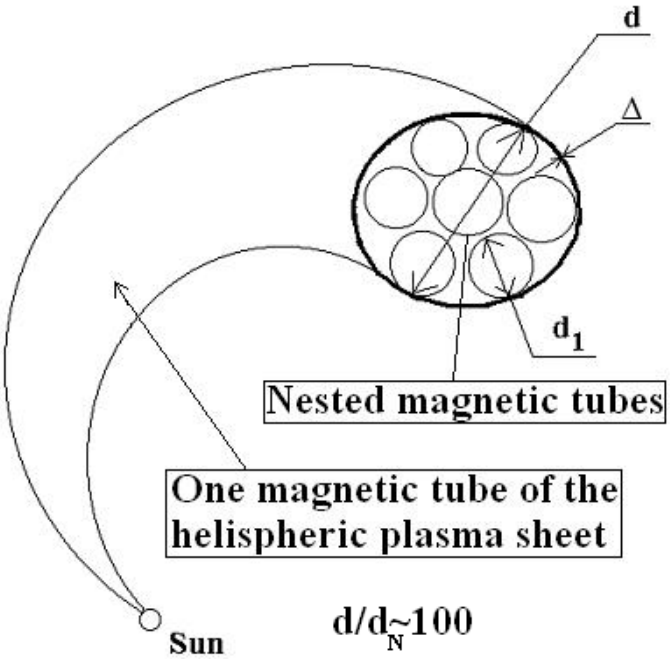

Fig. 6. The magnetic tube fractal structure in the solar wind according to the findings of **(V.G. Eselevich & M.V. Eselevich, 2005**).

The theory of possible evolution of such self-similar magnetic tubes (typical of fractal formations) in solar wind plasma was presented in (**Milovanov & Zelenyi, 1999**). However, no detailed comparison between the theoretical and experimental results has been made so far which is obviously necessary to understand the character of this interesting phenomena.

3. CME laws

Law 10. "Of the CME structure": The magnetic structure of a coronal mass ejection (CME) is a helical flux rope. In white-light images at a definite orientation to the sky plane, it can be seen as a bright frontal structure covering a cavity with a bright core.

It has been found that most CMEs with a big angular size (d > 30° - 50°) are helical flux ropes or tubes filled with plasma (**Krall et al., 2000**). This is supported by comparison between stereoscopic observation of CMEs with STEREO/SECCHI and calculations within the CME geometrical model in the form of a flux rope (**Thernisienet al., 2009**). According to (**Cremades & Bothmer, 2004**), axis orientation of the CME flux rope is nearly the same as the neutral line (NL) orientation near the CME source on the Sun or as the filament orientation along NL. The angle between NL and N-S direction on the Sun is denoted by γ. When observed in white light, "limb" CMEs in longitude $\Phi > 60°$, with high values $\gamma > 45°$, are of the simplest three-body form (**Illing & Hundhausen, 1985)**: frontal structure (FS), region of a lowered density (cavity), and a bright core that is sometimes absent.

Law 11. "Of the generation mechanism for "gradual" CMEs": The generation mechanism for "gradual" CMEs is associated with the development of instability in the magnetic flux rope with its top in the corona and two bases in the photosphere.

"Gradual" CMEs (Sheeley et al., 1999; V.G. Eselevich & M.V. Eselevich, 2011) have the following peculiarities:

- the corona is the source of the leading edge of these CMEs at $1.2R_0<R<2.5R_0$ from the solar centre;
- CMEs start moving from the state of rest; i.e., the initial velocity $V_0 = 0$;
- the initial angular size in the state of rest $d_0 \approx 15° - 65°$.

At zero time, a gradual CME is an arch structure of helical flux ropes, filled with plasma, with two bases in the solar photosphere. In theoretical papers (**Krall et al., 2000; Kuznetsov Hood, 2000**), the eruption or the sudden motion of the arch structure of flux rope (localised in the solar corona) backward from the Sun is considered as a source of gradual CMEs. In (**Krall et al., 2000**), four specific drive mechanisms for the flux rope eruption forming CMEs are considered:

(1) flux injection, (2) footpoint twisting, (3) magnetic energy release, and (4) hot plasma injection.

In (**Kuznetsov & Hood, 2000**), no flux-rope equilibrium is caused by the increase in plasma pressure in the rope due to plasma heating. All these models show that eruption of the magnetic flux rope is possible in principle. However, only experimental investigation, being in close cooperation with theory, will throw light upon real causes of this process.

Laws 10 and 11 may later merge.

Law 12. "Of a CME initiation site": CMEs appear in bases of the streamer belt or chains.

Fig. 7a illustrates that there are almost no streamer chains (dashed curves) near the minimum phase. All CMEs (their positions and angular sizes are depicted by segments of vertical straight lines) appear near NL (solid curve) along the streamer belt (**Hundhausen, 1993)**. Number of streamer chains increases as solar activity grows. CMEs appear in bases of the streamer belt (near NL) or chains (dashed line) Fig. 7b,c,d (**V.G. Eselevich, 1995**).

Law 13. "Of a disturbed region in front of CME": Owing to the interaction with coronal plasma there is a disturbed region in front of CME.

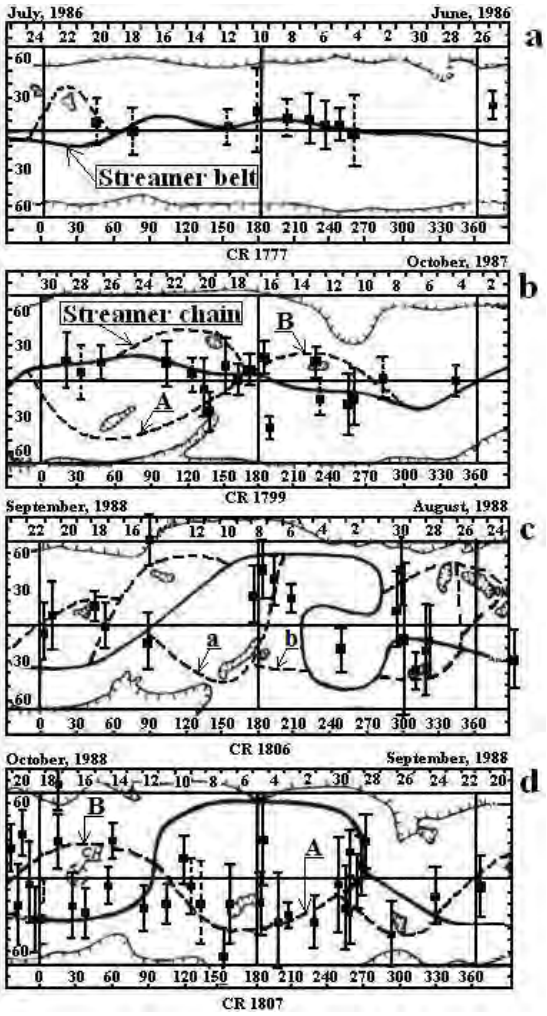

Fig. 7. Origin places of CME (vertical lines correspond to the CME angular size) relative to the streamer belt (solid curve is NL along the belt) and chains (dashed curve) for different Carrington rotations with an increase in solar activity from **(Eselevich, 1995)**.

The form of the frontal structure (FS) for the slow CME (its velocity relative to the undisturbed SW u < 700 km/s at R<6R_0) is close to the circle with radius "r" (shown dashed) centred at O (Fig.8A). This is confirmed by the coincidence between maxima of difference brightness distributions (see Fig. 8B) along two different directions (dashed lines 'a' and 'b' in Fig. 8A). For the slow SW the difference brightness profile is stretched in the CME propagation direction (Fig. 8B). This is a disturbed region arising from the interaction between CME and undisturbed SW (**M.V. Eselevich.& V.G. Eselevich, 2007a**). Examining the properties of the existing disturbed regions is important not only for understanding CME dynamics but also for identifying and studying the properties of the shock wave appearing in its front part at high velocities(u≥ 700 km/s) (see Law 15).

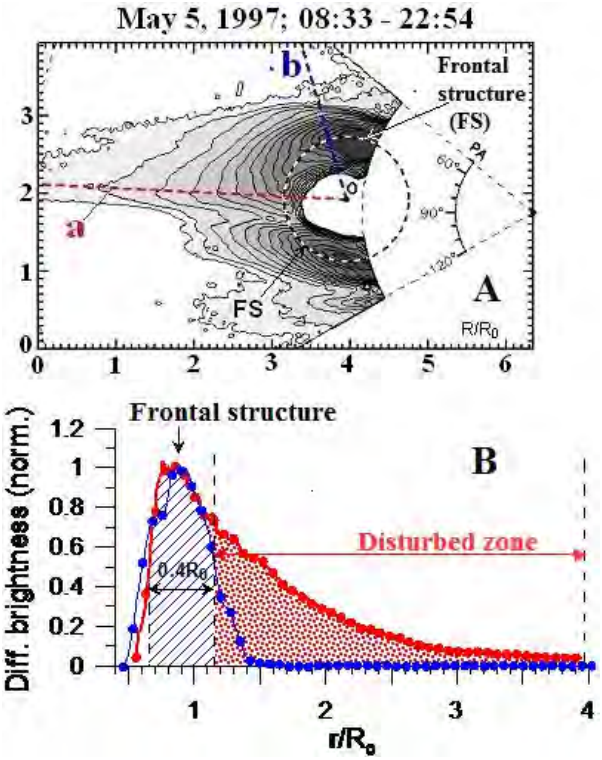

Fig. 8. (A) The difference brightness in the form of brightness isolines for the slow CME of 5 May 1997 (the velocity in reference to the undisturbed SW u ≈ 150 km/s). (B) The difference brightness profiles in the direction of two position angles (shown by dashed lines "a" (red) and "b"(blue) in (A). Value r is counted from the CME centre "O".

4. Shock wave problem. Laws of the CME-driven shock waves

4.1 Shock wave problem and its related law

First of all, let us divide this problem into two inequivalent components: collisional and collisionless shock waves.

Collisional shock waves. The waves are theoretically studied in gas (liquid) (Landau & Lifshitz, 1953) and plasma (Zeldovich & Riser, 1966). According to these studies, there are two main parameters of medium which are important for formation of the shock-wave discontinuity: velocity of sound (V_S) and mean free path (of gas or plasma) λ. It has been found experimentally (e.g., Korolev et al., 1978) that, as gas flow rate V exceeds value V_S, a shock wave discontinuity emerges where the Rankine-Hugoniot relations are valid. (This phenomenon is sometimes referred to as the "excess of velocity of sound"). As compared with gas, the structure of the shock front in plasma is complicated, since the scale where the ion heating takes place of the order of the mean free path for ions λ_i turns out different from the scale of heating for electrons $\lambda_e \sim (mi/me)^{1/2} \lambda_i$ (m_i and m_e are the ionic and electron masses, respectively) (Zeldovich & Riser, 1966). Experimental investigation into the structure of collisional shock front is, however, impossible because of small λ and λ_i in dense medium.

Collisionless shock waves. The situation gets worse in rarefied magnetised plasma which solar wind (SW) is. This can be explained by the fact that both parameters $\lambda_i = \lambda_p$ (λ_p is the mean free path of protons constituting SW) and V_S become, to a great extent, ambiguous for formation of the shock front, because λ_p in the Earth's orbit is of the order of the Sun-Earth distance. Apparently, the collisional shock wave with such a front thickness becomes meaningless. The second parameter (V_S) becomes indefinite, since V_S in magnetised plasma depends on the wave motion direction relative to the magnetic field direction. Fundamental theoretical works by R.Z. Sagdeev (review by Sagdeev, 1964) present the break in this deadlock. His research has shown that formation of the front with thickness $\delta << \lambda_p$ can be caused by collective processes in diluted plasma that are related to the development of an instability and its resulting plasma 'turbulisation'. As a consequence, the effective mean free path of protons dramatically decreases, being determined by the characteristic scale of the 'turbulence' $\delta_t << \lambda_p$. This scale plays the role of a new characteristic mean free path wherein the effective energy dissipation in the collisionless shock front may take place. So far, there has been no unified theory of front thickness in rarefied plasma that could explain various particular cases. There are numerous phenomena associated with collective processes.

Nevertheless, some limiting cases have not only been predicted theoretically (Sagdeev, 1964; Galeev and Sagdeev, 1966; Tidman, 1967) but also found in laboratory (Iskoldsky et al., 1964; Zagorodnikov et al., 1964; Paul et al., 1965; Alikhanov et al. 1968; Wong & Means, 1971; Volkov et al., 1974) and space experiments (Moreno et al., 1966; Olbert, 1968; Bame et al., 1979; Vaisberg et al., 1982). The comparison of the laboratory and satellite experiments has revealed a close agreement between them for certain collisionless shock fronts (V.G. Eselevich, 1983). Much experimental data on the structure of the near-Earth bow shock and interplanetary shock waves have been collected so far. There exists a possibility to analyse and interpret these data in order to deduce some experimental fundamental laws that will describe collective dissipation processes at the fronts of different collisionless shocks. Leaning on these laws, we will be able to elaborate a unified theory describing the front thickness in diluted plasma. However, these findings provide the basis for the law of collisionless shock existence given below.

Law 14. "Of the collisionless shock existence": The wave shocks with the front thickness being much smaller than the mean free path of ions and electrons may exist in rarefied plasma (The Sagdeev Law).

For some limiting cases, the collisionless shock has been predicted theoretically (**Sagdeev, 1964**). The existence of such waves has been proved both in laboratory (**Iskoldsky et al., 1964; Zagorodnikov et al., 1964; Paul et al., 1965**) and in the space plasma (**Moreno et al., 1966; Olbert, 1968**).

4.2 The CME-driven shock wave

The recent research into CME-driven shocks in the solar corona enabled us to deduce several new laws.

Law 15. "Of the formation of a shock in front of CME": A shock is formed in front of CME when its velocity relative to the surrounding coronal plasma exceeds the local Alfven one.

In the case of the fast CME (u ≥ 700 km/s), unlike in the case of the slow one (see Fig.8 B), the form of the difference brightness isolines is close to the frontal structure (FS) depicted by dashed circle in Fig. 9A. At the leading edge of the disturbed region in profile ΔP(R) (Fig. 9B),

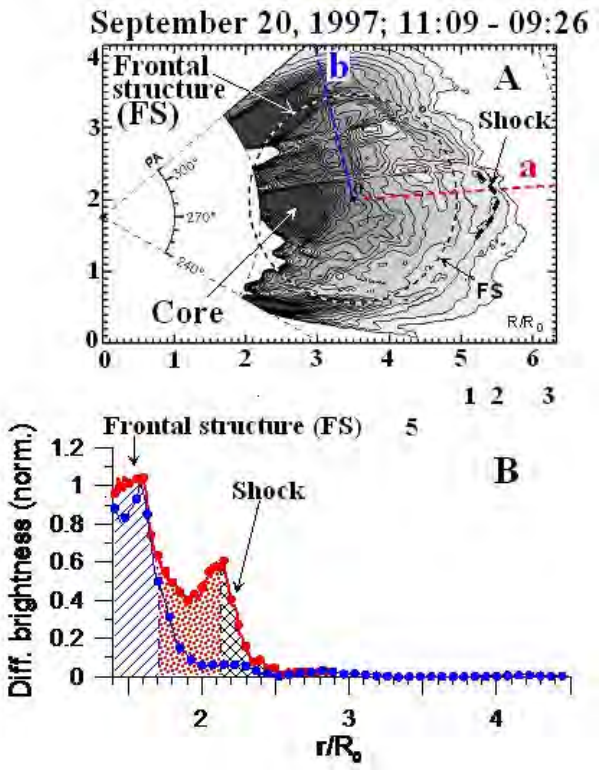

Fig. 9. The fast CME (u ≈ 700 km/s), 20 September 1997. (A) – Images in the form of difference brightness isolines ΔP, PA is the position angle; the coordinate axes are in units of R_0. (B) Difference brightness distributions with the distance r counted from the CME centre (point O) along two different sections "a"(red) and "b"(blue) whose directions are shown by the dashed lines in (A).

in the CME propagation direction (dashed straight line "a" in Fig.9A), there is a discontinuity (jump) with the scale of about 0.25 R_0 (inclined mesh). Fig.9A illustrates its position (segment of the heavy dashed curve).

The analysis (**M.V. Eselevich & V. G. Eselevich, 2008**) of dependence u(R) in Fig.10 allowed us to deduce the following law. When the CME propagation speed u, relative to surrounding coronal plasma, is lower than a certain critical speed u_C, there is a disturbed region extended along its propagation direction ahead of CME (these cases are highlighted by light marks). The formation of a shock ahead of the CME frontal structure in a certain vicinity relative to its propagation direction (events marked off by black marks) is determined by validity of the local inequality $u(R) > u_C \approx V_A(R)$ that can be true at different $R > 1.5R_0$ from the solar centre. Here, $V_A(R)$ is the local Alfven velocity of the slow SW in the streamer belt, calculated in (Mann et al., 1999) (green curve in Fig. 10). In the corona, V_A is approximately equal to the velocity of magnetic sound.

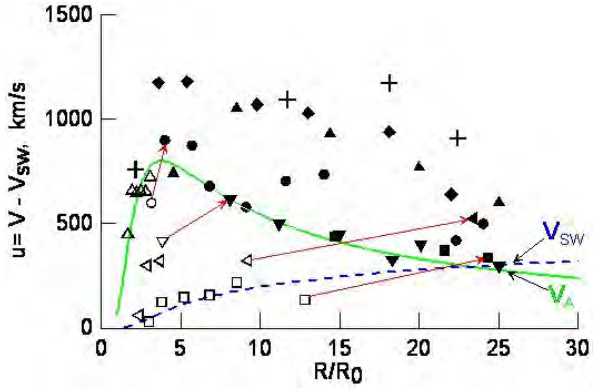

Fig. 10. The velocities "u" relative to the surrounding SW depending on the distance from the solar centre for the CME frontal structure (light marks) or the shock in front of CME (black marks) in the direction of propagation. The green curve is the Alfven velocity in the streamer belt from (Mann et al., 1999), the blue dotted curve is the velocity V_{SW} of the quasi-stationary, slow SW in the streamer belt from (Wang et al., 2000).

Law 16. "Of the transition from collisional to collisionless shock driven in front of CME": The energy dissipation mechanism at the front of a shock driven in front of CME at $R \leq 6R_0$ from the solar centre is collisional (R_0 is the solar radius). The transition from collisional to collisionless shock occurs at $R \geq 10R_0$.

According to (**M.V. Eselevich, 2010**), the front thickness δ_F of a CME-driven shock at $R \leq 6R_0$ increases with distance (the blue dashed curve in Fig. 11), remaining to be of order of the mean free path of protons λ_p (the two green dashed curves for coronal plasma temperature for $T = 10^6$K and $2 \bullet 10^6$K, respectively). This indicates at the collisional mechanism for energy dissipation at the shock front. At $R > 10\text{-}15R_0$, the formation of a new discontinuity having thickness $\delta_F^* << \lambda_p$ is observed at the shock front leading edge. The size of δ_F^* (within the measurement accuracy) does not vary with distance and is determined by the K spatial resolution of LASCO C3 ($K \approx 0.12R_0$) or STEREO/COR2 ($K \approx 0.03R_0$) in accordance with the data employed for these measurements. This implies that the real thickness is much

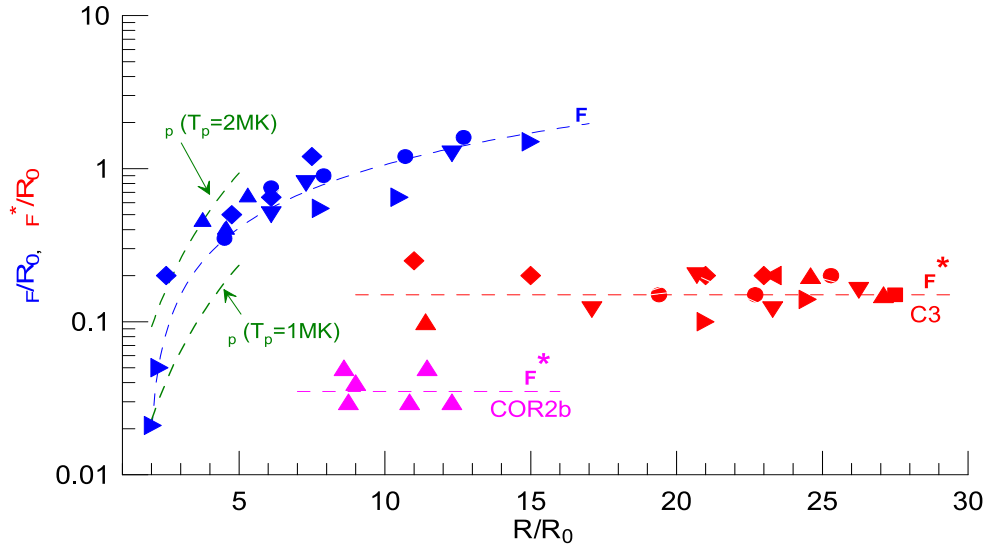

Fig. 11. The change in the CME-driven δ_F shock front thickness with distance R from the solar centre for seven different CMEs with high velocities. The calculated dependences: two green dashed curves show the mean free path of protons λp for two proton temperatures: T = 10^6 K and $2 \bullet 10^6$ K.. The blue dashed curve indicates the average thickness of the collisional shock front; the upper (red) and lower (violet) dashed lines stand for the average thickness of the collisionless shock front according to LASCO C3 and STEREO/COR2 data respectively from **(V.G. Eselevich, 2010)**.

less than the measured one (the image resolution is low), and the shock wave is apparently collisionless. To check this assumption, we have compared the dependence of the Alfven Mach number M_A on the shock wave strength ρ_2/ρ_1 with calculations within the ideal MHD for 10 shock waves (velocities being 800-2500 km/s) at the distance from $10R_0$ to $30R_0$ (**M.V. Eselevich & V.G. Eselevich, 2011**). As deduced from the comparison, the effective adiabatic index responsible for the processes at the front is within 2 to 5/3. This corresponds to the effective number of freedom degrees from 2 to 3 (Sagdeev, 1964). The similar dependence $M_A(\rho_2/\rho_1)$ has been obtained for the near-Earth bow shock and interplanetary collisionless shock waves. All these facts substantiate the assumption that the discontinuities under consideration, taking place in CME's leading edge at $R \geq 10\text{-}15R_0$, are really collisionless shock waves.

Law 17. "Of the blast shock driven by quite a powerful source of the sporadic SW (flares or CMEs)": A blast shock appears due to a pressure pulse resulting from quite a powerful flare or CME.

In the blast shock scenario (**Steinolfson et al., 1978**), the initial pressure pulse caused by a flare or a CME (**Uchida, 1968; Vrsnak & Lulic, 2000**) leads to excitation and propagation of a fast mode of the MHD wave in the corona. The mode transforms into a shock; the more powerful is the pressure pulse, the faster is the transformation. In the chromosphere, it has been first observed in the Hα line as the Moreton wave (**Moreton&Ramsey, 1960**); its manifestation in the corona is the so-called EIT wave (**Thompson et al., 1998**). The characteristic features

distinguishing the blast shock from other types of disturbances and waves are: deceleration, broadening, and decrease in intensity of the profiles (**Warmuth et al., 2001**)

Law 18. "Of the existence of "foreshock" in front of the collisionless shock front": There is a region of an increased turbulence –"foreshock" – ahead of the front of collisionless bow and interplanetary shocks.

The experiments have shown that there is a region of an increased turbulence - "foreshock" - ahead of the near-Earth bow shock front (**Asbridge et al., 1968; Lin et al., 1974; Lee, 1982**) and the CME-driven shock (**Scholer et al., 1983; Lee, 1983**). Even though having different excitation mechanisms and sizes in the heliosphere, their shock front structures and "foreshock" characteristic features are the same. But their most important common feature is the diffuse plasma acceleration in the "foreshock" (**Desai and Burgess, 2008**).

In (Eastwood et al., 2005) presents a generalised pattern of the "foreshock" ahead of the near-Earth bow shock with its peculiarities and comments. Even though considerable successes have been achieved in developing the "foreshock" theory, many questions (the complete list is given in (**Desai and Burgess, 2008**) are still unanswered.

Law 19. "Of two mechanisms for solar energetic particle acceleration": There are two different classes and hence two different mechanisms for acceleration of solar energetic particles: Impulsive - particles are accelerated in flares and recorded at 1 A.U. in a narrow range of solar longitude angles. Gradual - particles are accelerated by CME-driven shocks and recorded in a wide range of solar longitudes (of about 200°).

Over the last thirty years, many papers have been written on impulsive and gradual events of solar energetic particles (SEP) (e.g., Cliver, et al., 1982; Kahler, et al., 1984; Mason et al., 1984; Cane et al., 1986, etc.); the papers have contributed greatly to the substantiation of this law. In our brief description, we will rely on the papers (**Reams, 1990; 1999**) presenting these two events in their pure form. Impulsive SEPs are driven by powerful solar flares in the western solar hemisphere. Having a small Larmor radius, they propagate along the Earth-related magnetic lines of force of IMF over a relatively narrow longitude range $\Delta\Phi \approx (20° - 40°)$. Their time profile has a narrow peak with a characteristic width of several hours (**Reams, 1999**). Gradual SEPs appear near the shock, ahead of CME, and are recorded over a wide range of longitudes ≈ 200°. Their time profile has a wider peak of several days (**Reams, 1999**).

According to [Desai and Burgess, 2008], these differences imply that mechanisms of collective particle acceleration in two events are not the same: impulsive ones are characterized by stochastic acceleration of coronal plasma heated during the flare; gradual ones feature diffuse plasma acceleration driven by the shock ahead of CME. In the case of gradual SEPs, plasma acceleration driven by the shock takes place at the front and in the "foreshock" region whose structure is similar to that of the "foreshock" ahead of the near-Earth bow shock (law 18). The mechanism for particle acceleration in flares is less well understood. In reality, impulsive and gradual SEPs are usually observed simultaneously. That is why laying down law 19 is important to study such complicated situations.

Law 20. "Of the relationship between the type-II radio emission and collisionless shocks": Type-II radio bursts are associated with processes of Rayleigh and Raman scattering of random, Langmuir electron oscillations occurring in the shock front and in the "foreshock" of collisionless shocks.

According to (**Zheleznyakov, 1965; Zaitsev, 1965**), type-II radio bursts can be associated with processes of Rayleigh and Raman scattering of random, Langmuir oscillations occurring in the front of collisionless laminar shocks. Due to the revealing of an increased turbulence region – "foreshock" - ahead of the front of the near-Earth bow shock (Asbridge et al., 1968; Lin et al., 1974; Lee, 1982) and interplanetary shock (Scholer et al., 1983; Lee, 1983), the Zheleznyakov-Zaitsev Law has turned out more universal, since the number of instabilities (and, consequently, of collisionless shock fronts) capable of exciting random Langmuir oscillations has increased. Indeed, it has been found that there are flows of energetic particles (electrons and ions) in the foreshock of the near-Earth bow shock (**Cairms et al., 1987**) and in interplanetary shocks (**Bale et al., 1999**); the flows move along the front of the undisturbed magnetic field. They are the most energetic part of heated plasma in the shock front. The collective process heating the front is of no importance. Due to the development of beam instability, electron flows in the "foreshock" excite electrostatic oscillations at the electron plasma frequency. As a result of Rayleigh and Raman scattering, these oscillations transform into the first and second harmonics of the type-II radio emission at the single and double electron plasma frequencies, respectively (**Kuncic et al., 2002**). This process is confirmed by direct observations of the simultaneous appearance of an increased level of electrostatic Langmuir oscillations ahead of the shock front and of type-II radio bursts at the same frequencies (**Bale et al., 1999**).

Laws 18, 19, and 20 may later merge.

5. Conclusion

1. This paper is the first attempt to lay down SW laws, using research results over the past 40 years. This needs to be done because
   - These laws enable further investigations into SW not only as a chaotically changing medium studied usually by statistical methods, but also as a quasiregular medium satisfying certain laws. This determines the choice of future investigation methods, largely non-statistical.
   - These laws allow us to study causes of possible SW behaviour deviations from the laws in more complex situations as well as to discover new laws.
2. The proposed list of the 20 SW laws is incomplete and it is to stand the test of time.
3. Particular attention should be given to five laws (14, 15, 16, 17, 18) dealing with shock waves: there is no unified theory of the front thickness in plasma for them that could explain various particular cases, though the laws are qualitatively understandable and physically meaningful. These five laws are most universal among all those listed above. But their mechanisms are still unknown. This line of investigation is very fruitful for both solar-terrestrial physics and plasma physics.
4. Priority of collisionless shocks over other most topical issues of solar-terrestrial physics was discussed by Sagdeev, R.Z. (Sagdeev, 2010) and Russell, C.T. (Russell, 2010) in their invited reports at COSPAR 2010.
5. Such analysis-generalization should also be conducted for the Sun (though it has been partially done in many monographs) as well as for the Earth's magnetosphere and ionosphere in their own right.
6. Laying down the SW laws actually implies that the space science "solar wind" subdiscipline turns from multidirectional investigations and data collection into an independent branch of physics.

6. Acknowledgments

I would like to express our profound gratitude to Corr. Member of RAS Viktor M. Grigoryev: the bulk of our research has been done in Solar Physics Department headed by him. I am also thankful to Academician of RAS Geliy A. Zherebtsov for his support and encouragement, enabling us to fight through every hardship when preparing this paper. I am especially grateful to Academician of USSR AS Roald Z. Sagdeev who discovered collisionless shock waves 50 years ago. His infrequent but extremely useful e-mails have contributed greatly to this chapter, allowing us to improve it dramatically.

I thank O.Kulish, K. Korzhova and Yuri Kaplunenko for the help in translation in the English.

The work was supported the Russian Foundation for Basic Research (Projects No. 09-02-00165a, No.10-02-00607-a).

7. References

Alikhanov, S.G.; Belan, V.G. & Sagdeev, R.Z. (1968). Non-linear ion-acoustic waves in plasma. *JETP Letters.,* Vol. 7, pp. 465.

Asbridge, J.R.; Bame, S.J. & Srong, I.B. (1968). Outward flow of protons from the earth's bow shock. *J.Geophys.Res*, Vol.73, pp. 777.

Arge, C. N. & Pizzo, V. J. (2003). Improvement in the prediction of solar wind conditions using near-real time solar magnetic field updates. *J. Geophys. Res.*, V. 105, No. A5, pp. 10465-10479.

Bonetti A.; Bridge H.S., Lazarus A.J., Lyon E.F., Rossi R. &, Scherb F. (1963). Explorer 10 plasma measurements. *J. Geophys. Res*., Vol.68, pp. 4017-4063.

Belcher, J.W. & Davis, L. Jr. (1971). Large-amplitude Alfven waves in the interplanetary medium. 2, *J. Geophys. Res*., Vol.76, pp. 3534-3563.

Bame, S.J.; Asbridge, J.R., Gosling, J.T., Halbig, M., Paschmann G., Scopke, N. & Rosenbauer, H. (1979). High temporal resolution observations of electron heating at the bow shock. *Space Sci. Rev.,* Vol.23, pp. 75-92.

Burlaga., L. F. (1974). Interplanetary stream interfaces, *J. Geophys. Res*., Vol. 79, pp. 3717 – 3725.

Borrini G.; Wilcox, J. M., Gosling J. T., Bame S. J. & Feldman W. C. (1981). Solar wind helium and hydrogen structure near the heliospheric current sheet; a signal of coronal streamer at 1 AU. *J. Geophys. Res*. Vol.86. pp. 4565 -4573.

Burlaga, L.F.; Hundhausen, A.J. & Xue-pu Zhao. (1981). The coronal and interplanetary current sheet in early 1976. *J. Geophys. Res*., Vol. 86, pp. 8893 - 8898.

Bavassano B.; Woo, R. & Bruno, R. (1997). Heliospheric plasma sheet and coronal streamers. Geophys. Res. Let., Vol.24, pp. 1655 - 1658.

Bale, S.D.; Reiner, M.J., Bougeret, J.-L., Kaiser, M.L., Kruker, S., Larson, D.E. & Lin, R.P. (1999). The source region of an interplanetary type II radio burst. *Geophys. Res. Lett.*, Vol. 26, No.11, pp. 1573 - 1576.

Burton, M.E; Neugebauer, M., Crooker, N. U., von Steiger, R. & Smith, E.J. (1999). Identification of trailing edge solar wind stream interface: A comparison of Ulysses

plasma and composition measurements. J. Geophys. Res., Vol.104, No.A5, pp. 9925 - 9932.

Cliver, E.W.; Kahler, S.W., Shea, M.A. & Smart, D.F. (1982). Injection onsets of 2Gev protons, 1 MeV electrons in solar cosmic ray flare. *Astrophys. J.*, Vol.260, pp. 362-370, doi: 10.1086/160261.

Cane, H.V.; McGuire, R.E. & Rosenvinge, T.T. (1986). Two classes of solar energetic particle vents associated with impulsive and longduration soft X-ray flares. *Astrophys. J.*, Vol.301, pp. 448- 459, doi: 10.1086/163913.

Cairns, L.H. (1987). The electron distribution function upstream from the Earth's bow shock. *J. Geophys. Res.,* Vol.92, pp. 2315.

Cremandes, H. & Bothmer, V. (2004). On the three-dimensional configuration of coronal mass ejections. *Astronomy and Astrophysics*, Vol.422, pp. 307-332. DOI: 10.1051/0004-6361:20035776.

Dessler, A.J. &. Fejer, J.A. (1963). Interpretation of Kp- index and M-region geomagnetic storms. *Planet.Space Sci.*,Vol.11, pp. 505.

Desai, M.I. & Burgess, D. (2008). Particle acceleration at coronal mass ejection-driven interplanetary shocks and Earth's bow shock. *J.Geophys. Res*, Vol. 113, pp. A00B06, doi:10.1029/2008JA013219.

Eselevich, V.G. (1983). Bow shock structure from laboratory and satellite experimental results. *Planet. Spase Sci.,* Vol.34, No.11, pp. 1119-1132.

Eselevich, V. G. & Filippov, M.A. (1986). Study of the mechanism for solar wind formation. *Planet.Space Sci.*, Vol.34, No.11, pp. 1119-1132.

Eselevich, V.G.; Kaigorodov, A.P. & Fainshtein, V.G. (1990). Some peculiarities of solar plasma flows from coronal holes. *Planet. Space Si*. Vol. 38, No. 4, pp.459- 469.

Eselevich, V. G. (1992). Relationships of quasistationary solar wind flows with their sources on the Sun. *Solar Phys* ., Vol.137, pp. 179-197.

Eselevich, V.G. & Fainshtein, V.G. (1992). On the existence of the heliospheric current sheet without a neutral line (HCS without NL). *Planet. Space Sci.*, Vol.40, pp. 105 - 119.

Eselevich, V. G. (1995). New results on the site initiations of CMEs. *Geophys. Res. Let.*, Vol. 22 (20), pp. 2681 - 2684.

Eselevich, V.G. & Eselevich, M. V. (1999). An investigation of the fine ray structure of the coronal streamer belt using LASCO data. *Solar Phys*., Vol.188, pp. 299 - 313.

Eselevich, V.G.; Rudenko, V.G. & Fainshtein, V.G. (1999). Study of the structure of streamer bels and chains in the Solar corona. *Solar Phys*.,Vol.188, pp. 277 – 297. Eselevich, V. & Eselevich, M. (2002). Study of the nonradial directional property of the rays of the streamer belt and chains in the solar corona. *Solar Phys*., Vol.208, pp. 5 - 16.

Eselevich, V. G. & Eselevich M. V. (2005). Prediction of magnetospheric disturbances caused by a quasi-stationary solar wind. *Chin. Space Sci*., Vol.,25 (5), pp. 374 -382.

Eastwood, O.3.; Lucek, E.A., Mazelle, C., Meziane, K., Narita, Y., Pickett, J. & Treumann, R.A. (2005). The foreshock. *Space Sci., Rev*., Vol.118, pp. 41-94, doi: 10.1007/s11214-005-3824-3.

Eselevich, M. V. & Eselevich, V. G. (2005). Fractal. Structure of the heliospheric plasma sheet in the Earth's orbit. Geomagnetism and Aeronomy, Vol.45, No.3, pp. 326-336.

Eselevich, M.V. & Eselevich, V.G. (2006). The double structure of the coronal streamer belt. *Solar Phys.*, Vol.235, pp. 331 - 344.

Eselevich, M.V. & Eselevich, V.G. (2007a). First experimental studies a perturbrd zone preceding the front of a coronal mass ejection. *Astronomy Reports*, Vol.51, No. 111, pp. 947-954.

Eselevich, M.V. & Eselevich, V.G. (2007b). Streamer Belt in the Solar Corona and the Earth's Orbit. *Geomagnetism and Aeronomy*, Vol.47, No.3, pp. 291–298.

Eselevich, M.V. & Eselevich, V.G. (2008). On formation of a shock wave in front of a coronal mass ejection with velocity exceeding the critical one. *Geophys.Res.Let.*, Vol.35, pp. L22105.

Eselevich, V. G.; Fainshtein, V. G., Rudenko, G. V., Eselevich, M. V. & Kashapova, L. K. (2009). Forecasting the velocity of quasi-stationary solar wind and the intensity of geomagnetic disturbances produced by It. *Cosmic Research*, Vol.47, No.2, pp. 95–113.

Eselevich, M. V. (2010). Detecting the widths of shock fronts. Preceding coronal mass ejections. *Astronomy Reports*, Vol.54, No.2, pp. 173–183.

Eselevich, M.V. & Eselevich, V.G. (2011). Relations estimated at shock discontinuities txcited by coronal mass ejections. *Astronomy Reports*, Vol.55, No.4, pp. 359–373.

Eselevich, M.V. & Eselevich, V.G. (2011). On the mechanism for forming a sporadic solar wind, *Solar-Terrestrial Physics*. Issue17, pp. 127-136, RAS SB Publishers.

Gringauz K.I.; Bezrukikh V.V., Ozerov V.D. & Rybchinsky R.E. (1960). A study of interplanetary ionized gas, energetic electrons and corpuscular emission of the Sun, using three-electrode traps of charged particles aboard the second space rocket. *Reports of the USSR Academy of Sciences*, Vol.131, pp. 1301-1304.

Galeev, A. A. & Sagdeev, R.Z. (1966). *Lecture on the nonlinear theory of plasma*. pp. 38, Trieste, Italy.

Gosling, J. T.; Asbridge, J. R., Bame, S. J. & Feldman, W. C. (1978). Solar wind sreamer jnterfaces, *J. Geophys. Re*s., Vol.83, No.A4, pp. 1401 - 1412.

Gosling, J. T.; Borrini, G., Asbridge, J.R., Bame, S.J., Feldman, W.C. & Hansen, R.T. (1981). Coronal streamers in the solar wind at 1 a.u, *J. Geophys. Res.*, Vol.82, pp. 5438 - 5448.

Geiss J.; Gloeckler G. & von.Steiger, R. (1995). Origin of the solar wind composition data. *Space Science Reviews*, Vol.72, pp. 49-60.

Goldstein, B.E.; Neugebauer, M., Phillips, J.L., Bame, S., Goeling, J.T., McComas, D.,Wang, Y.-M., Sheeley, N.R., & Suess,S.T. (1996). Ulysses plasma parameters: latitudinal, radial, and temporal variations. *Astron.Astrophys*. Vol.316, pp. 296-303.

Gubchenko, V.M., Khodachenko, M.L., Biernat, H.K. , Zaitsev, V.V. & Rucker, H.O. (2004). On a plasma kinetic model of a 3D solar corona and solar wind at the heliospheric sheet, *Hvar Obs. Bull.*, Vol.28 (1), pp. 127.

Hundhausen, A.J. & Burlaga, L.F. (1975). A model for the origin of solar wind stream interfaces. *J. Geophys. Res.*, Vol.80, pp. 1845 - 1848.

Hoeksema J.T. (1984). *Structure and evolution of the large scale solar and heliospheric magnetic fields*. Ph. D. Diss. Stahford Univ.

Hundhausen, A.T. (1993). Sizes and locations of coronal mass ejections: SMM observations from 1980 and 1984 – 1989. *J.Geophys. Res* , Vol.98, pp. 13,177 – 13,200.

Iskoldsky A.M.; Kurtmullayev R.Kh., Nesterikhin Yu.E. & Ponomarenko A.G. (1964). Experiments in collisionless shock wave in plasma. *ZhETF,* Vol.47, No.2, pp. 774-776.

Illing, R.M. & Hundhausen, A.T. (1985). Disruption of a coronal streamer by an eruptive prominence and coronal mass ejection. *J. Geophys. Res*., Vol.90, pp. 275 - 282.

Ivanov K.; Bothmer V., Cargill P.J., Kharshiladze A., Romashets E.P. & Veselovsky I.S. (2002). Subsector structure of the interplanetary space. *Proc. The Second Solar Cycle and Space Whether Euroconference*, pp. 317, Vicvo Equense (Italy).

Korzhov N P. (1977). Large-scale three-dimensional structure of the interplanetary magnetic field. *Solar Phys*., Vol.55, pp. 505.

Korolev A.S.; Boshenyatov B.V., Druker I.G. & Zatoloka V.V. (1978). *Impulse tubes in aerodynamic studies*, pp. 5-80, Novosibirsk, "Nauka".

Kahler, S.W.; Sheeley, N.R.Jr., Howard, R.A., Michels, D.J., Koomen, M.J., McGuire, R.E., von Rosenvinge, T.T. & Reams, D.V. (1984). Associations between coronal mass ejections associated with impulsive solar energetic particle events. *J. Geophys. Res*, Vol.89, pp. 9683 - 9693, doi:10.1029/JA089iA11p09683.

Krall, J.; Chen, J. & Santoro, R. (2000). Drive mechanisms of erupting solar magnetic flux ropes. Astrophys. J., Vol.539, pp. 964-982.

Kuznetsov , V.D. & Hood, A.W. (2000). A phenomenological model of coronal mass ejection. Adv. Space Sci., Vol.26, No.3, pp. 539-542.

Kuncic, Z.; Cairns, I.H., Knock, S., & Robinson, P.A. (2002). A quantitative theory for terrestrial foreshock radio emission., *Geophys. Res. Lett*., Vol.29, No.8, pp. 2-1, CiteID 1161, DOI 10.1029/2001GL014524.

Landau L.D. & Livshits E.M. (1953). *The mechanics of continuous media*. State Publishing House of Theoretical and Technical Literature, Moscow.

Lin, R.P.; Meng, C.I. & Anderson, K.A. (1974). 30-100kev protons upstream from the earth's bow shock. *J.Geophys. Res*, Vol.79, pp. 489 - 498.

Lee, M.A. (1982). Coupled hydromagnetic wave excitation and ion acceleration upstream of the Earth's bow shock. *J.Geophys. Res*, Vol.87, pp. 5063 - 5080.

Lee, M.A. (1983). Coupled hydromagnetic wave excitation and ion acceleration at interplanetary traveling shocks. *J.Geophys. Res*., Vol. 88, No. A8, pp. 6109-6119.

Moreton, G. E. & Ramsey, H. E. (1960). Recent Observations of Dynamical Phenomena Associated with Solar Flares. *PASP*, Vol. 72, pp. 357.

Moreno, G.; Olbert, S. & Pai, L. (1966). Risultati di Imp-1 sul vento solare. *Quad. Ric. Sci*., Vol.45, pp. 119.

Mason, G.M.; Gloecker, G. & Hovestadt, D. (1984). Temporal variations of nucleonic abundances in sllar flare energetic particle events. II – Evidence for large-scale shock acceleration. *Astrophys. J*., Vol.280, pp. 902 - 916, doi: 10.1086/162066/261.

Mann, G.; Aurass, H., Klassen, A., Estel, C. & Thompson, B. J. (1999). Coronal Transient Waves and Coronal Shock Waves. In: Vial, J.-C., Kaldeich-Schumann, B. (eds.*) Proc. 8th SOHO Workshop Plasma Dynamics and Diagnostics in the Solar Transition Region and Corona*, pp. 477-481, Paris, France, 22-25 June 1999.

Milovanov A. V. & Zelenyi L. M. (1999). Fraction excititations as a driving mechanism for the self-organized dynamical structuring in the solar wind. *Astrophys. Space Science*, Vol.264, pp. 317 - 345.

McComas, D. J. ; Elliott, H. A.; von Steiger, R. (2002). Solar wind from high latitude CH at solar maximum. *Geophys. Res. Lett.* Vol.29(9), pp. 28-1, CiteID 1314, DOI 10.1029/2001GL013940

Nolte, J.T.; Kriger A.S., Timothy, A.F., Gold, R.E., Roelof, E.C., Vaina, G., Lazarus, A.J., Sullivan, J.D. & Mcintosh, P.S. (1976). Coronal holes as sources of solar wind. *Solar Phys*., Vol.46, pp. 303-322.

Olbert, S. (1968). Summary of experimental results from MIT detector on Imp-1. *In Physics of Magnetosphere*, edited by R.L.Carovillano et al., p. 641, D.Reidel, Dordrecht, Netherland.

Ponomarev E.A. (1957). *On the theory of the solar corona*. Ph.D. Thesis in Physics and Mathematics. Kiev, Kiev University.

Parker E.N. (1958). Dynamics of interplanetary gas and magnetic fields. *Astrophys. J.*, Vol.128, pp. 664–675.

Sagdeev R.Z. (1964). Collective processes and shock waves in rarefied plasma, *Reviews of Plasma Physics*, Vol.2, pp. 20-80, M.: "Gosatomizdat".

Paul, J.W.H.; Holmes, l.S., Parkinson, M.J. & Sheffield, J. (1965). Experimantal observations on the structure of collisionless shock waves in a magnetized plasma. *Nature*, Vol.2, pp. 367-385.

Reams, D.V. (1990). Acceleration of energetic particles by shock waves from large solar flares, *Astrophys. J*, Vol.358, pp. L63 – L67.

Reams, D.V. (1999). Particle acceleration at the Sun and the heliosphere. *Space Sci. Rev*., Vol.90, pp. 413 - 491.

Russell, C. T. (2010). Advances in understanding the plasma physics of the solar wind: contributions from STEREO. *Theses of the report COSPAR 2010*. D33- 0002-10.

Svalgaard, L.J.; Wilcox, W. & Duvall, T.L. (1974). A model combining the solar magnetic field. *Solar Phys*., Vol.37, pp. 157 - 172.

Steinolfson, R. S.; Wu, S. T., Dryer, M. & Tanberg-Hanssen, E. (1978). Magnetohydrodynamic models of coronal transients in the meridional plane. I – The effect of the magnetic field, *Astrophys. J.*, Vol.225, pp. 259 - 274.

Scholer, M.; Ipavich, F.M. , Gloecker, G. & Hovestadt, D. (1983) Acceleration of low-energy protons and alpha particles at interplanetary shock waves . *J. Geophys. Res*., Vol.88, pp. 1977 - 1988.

Schwenn, R. & Marsch, E. (1991). *Physics of the inner heliosphere v. I and v. II,* Springer Verlag, pp. 185, Berlin Heidelberg,.

Sheeley, N.R.Jr.; Walter, H., Wang, Y.-M. & Howard, R.A. (1999). Continuous tracking of coronal outflows: Two kinds of coronal mass ejections, *J.Geophys. Res.* Vol.104, pp. 24739 - 24768.

Sagdeev, R. Z. (2010). The role of space as an open physics lab in enriching of plasma science. *Theses of the report COSPAR 2010.* (D33-0001- 10)

Tidman, D.A. (1967). Turbulent shock waves in plasma. *Phys. Fluids*, Vol.10, pp. 547-568.

Tompson, B.J.; Plunkett, S. P., Gurman, J. B., Newmark, J. S., St. Cyr, O. C.. & Michels, D. J. (1998). SOHO/EIT observations of an Earth-directed coronal mass ejection on May 1997, *Geophys. Res. Lett*., Vol.25, pp. 2465 - 2468.

Tlatov, A.G. & Vasil'eva, V.V. *(* 2009). The non-radial propagation of coronal streamers in minimum activity epoch. *Proceedings of the International Astronomical Union*, Vol.5, pp. 292.

Thernisien A., Vourlidas, A. and Howard, R.A. (2009). Forward modeling TEREO/SECCHI data. *Sol. Phys*., Vol.256, pp. 111- 130.

Uchida, Y. (1968). Propagation of hydromagnetic disturbances in the solar corona and Moreton's wave phenomenon, *Solar Phys*., Vol.4, pp. 30.

Vsekhsvyatsky S.K.; Ponomarev E.A., Nikolsky G.M. & Cherednichenko V.I. (1957). *On corpuscular emission. "Physics of solar corpuscular streams and their impact on the Earth's upper atmosphere"*, M., Publishing House of the USSR Academy of Sciences.

Volkov O.L.; Eselevich V.G., Kichigin G.N. & Paperny V.L.(1974). Turbulent shock waves in rarefied nonmagnetised plasma. *JETP*, Vol.67, pp. 1689-1692.

Vaisberg O.L.; Galeev A.A., Klimov S.I., Nozdrachev M.N., Omelchenko A.N. & Sagdeev R.Z. (1982). Study of energy dissipation mechanisms in collisionless shocks with high Mach numbers with the help of measurement data aboard the 'Prognoz-8' satellite. *JETP Letters*, Vol.35, pp. 25 .

Vrsnak, B., & Lulic.S. (2000). Formation of coronal MHD shock waves - II. The Pressure Pulse Mechanism, *Solar Phys*., Vol.196, pp. 181.

Wong, A.Y. & Means, R.W.(1971). Evolution of turbulent electrostatic shock. *Phys. Rev. Letters,* Vol.27, No.15, pp. 973-976.

Wilcox, John M. & Hundhausen, A.T. (1983). Comparison of heliospheric current sheet structure obtained from potential magnetic field computations and from observed polarization coronal brightness. *J. Geophys. Res*., Vol.88, pp. 8095 - 8086.

Wang Y.-M. & Sheeley, N. R. Jr. (1990). Solar wind speed and coronal flux-tube expansion *Astrophys. J.,* Vol.355, pp. 727-732.

Winterhalter D.; Smith E. J., Burton M. E. & Murphy N. (1994). The heliospheric plasma sheet. *J. Geophys. Res*., Vol.99, pp. 6667 - 6680.

Wang, Y.-M. (1995). Empirical relationship between the magnetic field and the mass and energy flux in the source regions of the solar wind. *Astrophys. J.*,Vol.449, pp. L157-L160.

Wang, Y.-M.; Sheeley, N. R., Socker, D. G., Howard, R. A. & Rich, N. B.(2000). The dynamical nature of coronal streamers. *J. Geophys. Res*., Vol.105, No.A11, pp. 25133-25142, DOI:10.1029/2000JA000149

Warmuth, A.; Vrsnak, B., Aurass, H.& Hanslmeier. (2001). Evolution of EIT/Hα Moreton waves, *Astrophys. J.*, Vol.560, pp. L105.

Wang, Y.M.; Sheeley, N.R. & Rich. N.B. (2007). Coronal pseudostreamers. *Astrophys. J.,* Vol. 685, pp. 1340 - 1348.

Zagorodnikov, S.P.; Rudakov, L.I., Smolkin, G.E. & Sholin.,G.V. (1964). Observation of shock waves in collisionless plasma. *JETP*, Vol.47, No.5, pp. 1770-1720.

Zheleznyakov, V. (1965). On the genesis of solar radio bursts in a metre wave range. *Astron. Journal [in Russian]*, Vol.XLII, pp. 244 – 252.

Zaitsev, V.V. (1965). On the theory of type-II solar radio bursts. *Astron. Journal [in Russian],* Vol. XLII, pp. 740 - 748.

Zeldovich, Ya. B. & Raiser, Yu.P. (1966). *Physics of shock waves and high-temperature hydrodynamic phenomena [in Russian],* pp. 398 – 406, Publishing House 'Nauka', Moscow.

Zhao, X. P. & Webb, D.F. (2003). Source regions and storm effectiveness of frontside full halo coronal mass ejections. *J.Geophys. Res.*, Vol..108, No.A6, pp. SSH4-1, CiteID 1234, DOI 10.1029/2002JA009606.